

# POLARIZATION OF THE MICROWAVE BACKGROUND: THEORETICAL FRAMEWORK

ALESSANDRO MELCHIORRI AND NICOLA VITTORIO

*Dipartimento di Fisica  
Università "Tor Vergata", Roma, Italy*

## **Abstract.**

We present a brief review of the polarization properties of the cosmic microwave background in dark matter models for structure formation. Quite independently of the model parameters, the polarization level is expected to be  $\sim 10\%$  of the anisotropy signal at angular scales  $\leq 1^\circ$ . Detections of polarization at larger angular scales would provide a strong evidence in favour of an early reionization of the intergalactic medium.

## **1. Introduction: some historical remarks**

Most of the early theoretical work on the polarization of the Cosmic Microwave Background (CMB) was focused, after Rees pioneering work [1], on anisotropic cosmological models [2,3,4,5,6,7,8,9]. The degree of Faraday rotation expected in the presence of an universal magnetic field and the use of polarization measurements to constraint the amplitude of such field were also considered [14,33]. More recently, it has been shown that even in isotropic cosmological models the anisotropic component of the CMB is polarized [10]. Detailed numerical predictions have been made for dark matter dominated models with adiabatic fluctuations [see e.g. 11,12,13], with and without an early reionization of the intergalactic medium [15]. These calculations have shown that the level of polarization can be 10 percent of the anisotropy signal. After the COBE/DMR result [16], new attention has been dedicated to the tensor modes of metric fluctuations, which also produces anisotropy on large angular scales [17,18,19,20,21,22,23]. The polarization due to a background of primordial gravitational waves has been widely discussed [24,25,26,27,28]. For describing the statistic of the polarization field was also introduced the polarization - anisotropy correlation

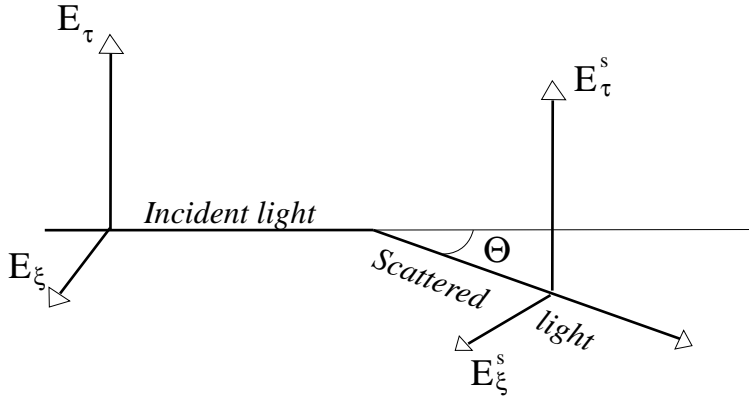


Figure 1. Thomson scattering of a photon by an electron.

function [29,30], while other authors [31,32] have shown that neglecting polarization yields a theoretical overestimate of the anisotropy at small angular scale.

From the experimental side, in spite of a continuous increment in the experimental sensitivity, no polarization was found and only upper limits were given [34,35,36,37], with the best upper limit to date of  $\sim 25\mu K$  from the Saskatoon experiment [38]. As we show in Section 5, the level of CMB polarization expected is in most of the models at least a factor 10 below this limit, so is not clear if the present sensitivity of the CMB experiments is sufficient to detect polarization. However, in view of forthcoming high sensitivity new experiments, it is of interest to discuss the general properties of the polarization pattern and its dependence to the various cosmological parameters. So, the aim of this work is to review the basics steps behind the theoretical calculation of CMB polarization. The plan of the paper is as follows. In Section 2 we briefly review the definition of the Stokes parameters and their variations in a Thomson scattering. In Section 3 and 4 we write the set of equations necessary to describe anisotropy and polarization of the CMB. In Section 5 we review some of the results obtained by numerically integrate those equations. Finally, in Section 6, we summarize the main findings.

## 2. An Elementary Description of the Polarization of Light

For an elliptically polarized wave, the components of the electric field along two orthogonal directions,  $\xi$  and  $\tau$  say, can be written as :

$$\begin{cases} E_\xi = E_\xi^0 \sin(\omega t - \epsilon_1) \\ E_\tau = E_\tau^0 \sin(\omega t - \epsilon_2) \end{cases} \quad (1)$$

where  $E_{\xi,\tau}^0$  and  $\epsilon_{1,2}$  are constants. The polarization of the radiation field is conveniently described in terms of the Stokes parameters :

$$\begin{cases} I = E_\xi^{02} + E_\tau^{02} \equiv I_\xi + I_\tau \\ Q = E_\xi^{02} - E_\tau^{02} \equiv I_\xi - I_\tau \\ U = 2E_\xi^0 E_\tau^0 \cos[\epsilon_1 - \epsilon_2] \\ V = 2E_\xi^0 E_\tau^0 \sin[\epsilon_1 - \epsilon_2] \end{cases} \quad (2)$$

The parameter  $I$  is proportional to the intensity of the wave (we omit the proportionality factor)  $V$  measures the ratio of the principal axes of the polarization ellipse while  $Q$  or  $U$  measures the orientation of the ellipse relative to the  $\xi$  axes. In general  $I^2 \geq Q^2 + U^2 + V^2$ , the equality holding for an elliptically polarized wave.

A clockwise rotation by an angle  $\Xi$  of the  $\xi - \tau$  axes in the polarization plane leaves unchanged the  $I$  and  $V$  parameters and it is equivalent to apply the operator:

$$\hat{\mathbf{L}}(\Xi) = \begin{pmatrix} \cos^2 \Xi & \sin^2 \Xi & \frac{\sin 2\Xi}{2} & 0 \\ \sin^2 \Xi & \cos^2 \Xi & -\frac{\sin 2\Xi}{2} & 0 \\ -\sin 2\Xi & \sin 2\Xi & \cos 2\Xi & 0 \\ 0 & 0 & 0 & 1 \end{pmatrix} \quad (3)$$

to the vector  $\vec{I} \equiv (I_\xi, I_\tau, U, V)$ .

In the Thomson scattering, the light scattered in a direction making an angle  $\Theta$  with the direction of incidence (see Figure 1) is

$$\begin{cases} E_\xi^s = \sqrt{\frac{3}{2}\sigma_T} E_\xi^0 \cos \Theta \sin(\omega t - \epsilon_1) \\ E_\tau^s = \sqrt{\frac{3}{2}\sigma_T} E_\tau^0 \sin(\omega t - \epsilon_2) \end{cases} \quad (4)$$

In analogy with the equation (2) the Stokes parameters of the scattered light are:

$$\begin{cases} I_\xi^s = (3/2)\sigma_T I_\xi \cos^2 \Theta \\ I_\tau^s = (3/2)\sigma_T I_\tau \\ U^s = (3/2)\sigma_T U \cos \Theta \\ V^s = (3/2)\sigma_T V \cos \Theta \end{cases} \quad (5)$$

or, in matrix form,  $\vec{I}^s = \sigma_T \hat{R} \times \vec{I}$ , where

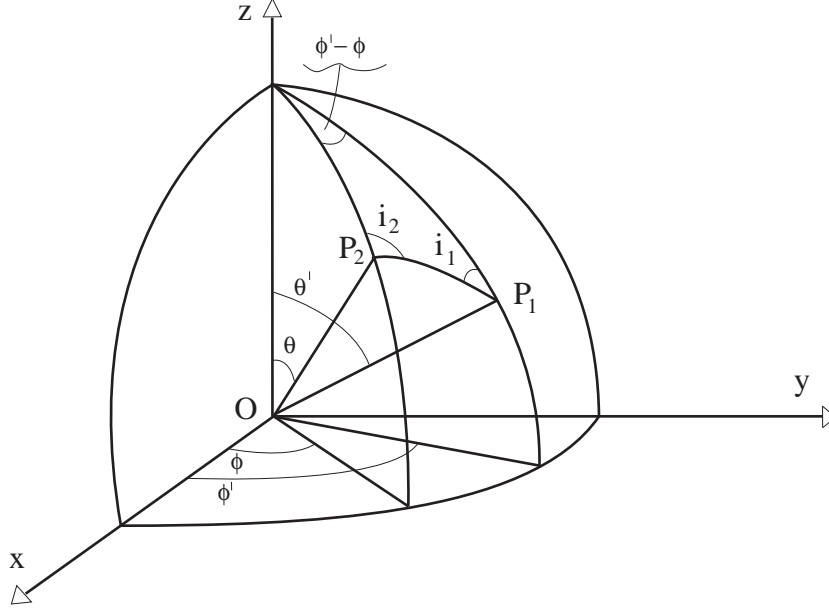


Figure 2. Coordinate system needed to describe Thomson scattering in the Lab frame.

$$\hat{R} = \frac{3}{2} \begin{pmatrix} \cos^2 \Theta & 0 & 0 & 0 \\ 0 & 1 & 0 & 0 \\ 0 & 0 & \cos \Theta & 0 \\ 0 & 0 & 0 & \cos \Theta \end{pmatrix} \quad (6)$$

In order to study the variations of Stokes parameters in the Lab frame (see Figure 2) we have to :

1. apply the transformation  $\hat{L}(-i_1)$  to  $\vec{I}$ , where  $i_1$  is the angle between the meridian and the scattering planes. In this way we obtain the Stokes parameters of the incident light in the frame of Figure 1.
2. apply  $\hat{R}$  to these parameters in order to obtain the Stokes parameters of the scattered light, again in the frame of Figure 1.
3. apply the transformation  $\hat{L}(\pi - i_2)$ , where  $i_2$  represents the angle between the plane  $OP_2Z$  and  $OP_1P_2$ . In this way we are back to the Lab frame.

Thus, the radiation scattered in the  $(\theta, \phi)$  direction, relative to the Lab frame, can be written as [39]:

$$\vec{I}^s(\theta, \phi) = \frac{1}{4\pi} \int_{4\pi} [\hat{P}(\theta, \phi; \theta', \phi') \times \vec{I}(\theta', \phi')] d\Omega' \quad (7)$$

where

$$\hat{P} = \hat{Q} \times [\hat{P}^0(\mu, \mu') + \sqrt{(1 - \mu^2)}\sqrt{(1 - \mu'^2)}\hat{P}^1(\mu, \phi, \mu', \phi') + \hat{P}^2(\mu, \phi, \mu', \phi')] \quad (8)$$

$$\hat{Q} = \begin{pmatrix} 1 & 0 & 0 & 0 \\ 0 & 1 & 0 & 0 \\ 0 & 0 & 2 & 0 \\ 0 & 0 & 0 & 2 \end{pmatrix}, \quad (9)$$

$$\hat{P}^0 = \frac{3}{4} \begin{pmatrix} 2(1 - \mu^2)(1 - \mu'^2) + \mu^2\mu'^2 & \mu^2 & 0 & 0 \\ \mu'^2 & 1 & 0 & 0 \\ 0 & 0 & 0 & 0 \\ 0 & 0 & 0 & \mu\mu' \end{pmatrix}, \quad (10)$$

$$\hat{P}^1 = \frac{3}{4} \begin{pmatrix} 4\mu\mu' \cos(\phi - \phi') & 0 & 2\mu \sin(\phi' - \phi) & 0 \\ 0 & 0 & 0 & 0 \\ -2\mu' \sin(\phi - \phi') & 0 & \cos(\phi - \phi') & 0 \\ 0 & 0 & 0 & \cos(\phi - \phi') \end{pmatrix}, \quad (11)$$

$$\hat{P}^2 = \frac{3}{4} \begin{pmatrix} \mu^2\mu'^2 \cos 2(\phi' - \phi) & -\mu^2 \cos 2(\phi' - \phi) & \mu^2\mu' \sin 2(\phi' - \phi) & 0 \\ -\mu'^2 \cos 2(\phi' - \phi) & \cos 2(\phi' - \phi) & -\mu' \sin 2(\phi' - \phi) & 0 \\ -\mu'^2\mu \sin 2(\phi' - \phi) & \mu \sin 2(\phi' - \phi) & \mu'\mu \cos 2(\phi' - \phi) & 0 \\ 0 & 0 & 0 & 0 \end{pmatrix}, \quad (12)$$

and  $\mu$  and  $\mu'$  are defined as  $\cos \theta$  and  $\cos \theta'$ , respectively.

### 3. The Boltzmann Transfer Equation for Polarized Light

In order to study anisotropy and polarization of the CMB we need to write down the transfer equation for the Stokes parameters. We restrict ourselves to isotropic universes where, to zero-th order, anisotropy and polarization vanish. The perturbations to the Stokes parameters and to the other relevant quantities (see section 3.3) are written in the synchronous gauge formalism. Following Peebles [40,41] we introduce the fractional fluctuations of the Stokes parameters as follows:

$$\begin{pmatrix} I \\ Q \\ U \\ V \end{pmatrix} = \frac{\rho_\gamma(t)}{4\pi} \begin{pmatrix} 1 + \iota \\ q \\ u \\ v \end{pmatrix} \quad (13)$$

where  $(\iota, q, u, v)$  are functions of the observer position  $\vec{x}$ , of the line of sight observation  $\hat{\gamma} \equiv (\gamma_1, \gamma_2, \gamma_3)$  and of the cosmic time  $t$ . To first order the transfer equations becomes

$$\frac{\partial}{\partial t} \begin{pmatrix} \iota \\ q \\ u \\ v \end{pmatrix} + \frac{\gamma_\alpha}{a} \frac{\partial}{\partial x^\alpha} \begin{pmatrix} \iota \\ q \\ u \\ v \end{pmatrix} + \begin{pmatrix} y \\ 0 \\ 0 \\ 0 \end{pmatrix} = \sigma_T n_e \left[ \begin{pmatrix} \iota^s \\ q^s \\ u^s \\ v^s \end{pmatrix} - \begin{pmatrix} \iota \\ q \\ u \\ v \end{pmatrix} \right] \quad (14)$$

where  $y = -2\dot{h}_{\alpha\beta}\gamma_\alpha\gamma_\beta$  is the term containing the linear perturbation to the metric tensor,  $(\iota^s, q^s, u^s, v^s)$  are evaluated in the comoving frame and refer to the radiation scattered in the  $\vec{\gamma}$  direction, and  $a$  is the scale factor. In order to avoid spatial dependence it is convenient to work in Fourier space. We choose for each  $k$  mode a reference system with the  $z$  axis parallel to  $\vec{k}$ , in order to achieve an azimuthal symmetry.

### 3.1. SCALAR MODES

For scalar modes, the only non vanishing components of the perturbed metric tensor are the diagonal ones :  $h_{11}, h_{22}, h_{33}$  ( $h_{00} \equiv 0$  because of the chosen gauge). Thus, the gravitational term in equation (14) has the form:  $y = (1 - 3\mu^2)\dot{h}_{33} - (1 - \mu^2)\dot{h}$ , and each Fourier mode is independent of the azimuthal angle  $\phi$ . After integrating over this angle equation (7) it can be proved that  $\hat{P}^1$  and  $\hat{P}^2$  give no contribution. Therefore we can assume  $U = 0$  in this case. Also the equation for  $V$  is decoupled from the others: if  $V$  vanishes at the beginning, it also vanishes afterwards. Therefore only the perturbations  $\iota$  and  $q$  of the  $I$  and  $Q$  parameters are of interest. Their evolution is described by the following transfer equation [10,11,12,13]:

$$\frac{\partial}{\partial t} \begin{pmatrix} \iota \\ q \end{pmatrix} + \frac{ik\mu}{a} \begin{pmatrix} \iota \\ q \end{pmatrix} - \begin{pmatrix} y \\ 0 \end{pmatrix} = \sigma_T n_e \left( \int_{-1}^1 \hat{M}_S(\mu, \mu') \begin{pmatrix} \iota' \\ q' \end{pmatrix} d\mu' - \begin{pmatrix} \iota + 4\mu v_b \\ q \end{pmatrix} \right) \quad (15)$$

where  $y = (1 - 3\mu^2)\dot{h}_{33} - (1 - \mu^2)\dot{h}$  is the term taking into account the effects of gravitational potential, and where the  $2 \times 2$  matrix  $\hat{M}_S$  is composed by the first two rows and columns of the matrix  $\hat{P}^0$  in the  $(I, Q, U, V)$  basis:

$$\hat{M}_S(\mu, \mu') = \frac{3}{16} \begin{pmatrix} 3 - \mu'^2 - \mu^2 + 3\mu^2\mu'^2 & 1 - \mu'^2 - 3\mu^2(1 - \mu'^2) \\ 1 - 3\mu'^2 - \mu^2 + 3\mu^2\mu'^2 & 3 - 3\mu'^2 - 3\mu^2(1 - \mu'^2) \end{pmatrix} \quad (16)$$

The angular dependence in equation (15) can be eliminated by expanding  $\iota$  and  $q$  in Legendre polynomials :

$$\iota = \sum_{\ell} (\sigma_{2\ell}^k(t) P_{2\ell}(\mu) + i\sigma_{2\ell+1}^k(t) P_{2\ell+1}(\mu)) \quad (17)$$

$$q = \sum_{\ell} (\eta_{2\ell}^k(t) P_{2\ell}(\mu) + i\eta_{2\ell+1}^k(t) P_{2\ell+1}(\mu)) \quad (18)$$

Because of the orthogonality of the Legendre polynomials, equation (15) becomes:

$$\begin{cases} \frac{\partial \iota}{\partial t} + \frac{ik\mu}{a}\iota - y_S = \sigma_T n_e \left( \sigma_0 - 4\mu v_b - \iota + P_2(\mu) 1/2(\sigma_2/5 - \eta_0 + \eta_2/5) \right) \\ \frac{\partial q}{\partial t} + \frac{ik\mu}{a}q = \sigma_T n_e \left( -q + 1/2(1 - P_2(\mu))(-\sigma_2/5 + \eta_0 - \eta_2/5) \right) \end{cases} \quad (19)$$

These equations are coupled together through the quadrupole term, *i.e.* the radiation must have a quadrupole anisotropy to get polarized.

### 3.2. TENSOR MODES

For tensor perturbations the only non vanishing components of the perturbed metric tensor are  $h_{11} = h_{22} = h_+$  and  $h_{12} = h_{21} = h_{\times}$  where the two values  $h_+$ ,  $h_{\times}$  refer to the two polarization states of the gravitational waves. The equation of transfer has the following form [24] :

$$\frac{\partial}{\partial t} \begin{pmatrix} \iota \\ q \\ u \end{pmatrix} + \frac{ik\mu}{a} \begin{pmatrix} \iota \\ q \\ u \end{pmatrix} - \begin{pmatrix} y \\ 0 \\ 0 \end{pmatrix} = \sigma_T n_e \left( \int_{\Omega} \hat{M}_T(\mu, \phi; \mu', \phi') \begin{pmatrix} \iota' \\ q' \\ u' \end{pmatrix} \frac{d\Omega'}{4\pi} - \begin{pmatrix} \iota \\ q \\ u \end{pmatrix} \right) \quad (20)$$

where now  $y = -\dot{h}_+(1 - \mu^2) \cos(2\phi) + \dot{h}_{\times}(1 - \mu^2) \sin(2\phi)$ , and the  $3 \times 3$  matrix  $\hat{M}_T$  is composed by the first three rows and columns of the matrix  $\hat{P}^2$  in the  $(I, Q, U, V)$  basis:

$$\hat{M}_T = \frac{3}{8} \begin{pmatrix} K_-(\mu)K_-(\mu') \cos \Delta_{\phi} & -K_-(\mu)K_+(\mu') \cos \Delta_{\phi} & -2\mu'K_-(\mu) \sin \Delta_{\phi} \\ K_+(\mu)K_-(\mu') \cos \Delta_{\phi} & -K_+(\mu)K_+(\mu') \cos \Delta_{\phi} & 2\mu'K_+(\mu) \sin \Delta_{\phi} \\ \mu K_-(\mu') \sin \Delta_{\phi} & -\mu K_+(\mu') \sin \Delta_{\phi} & 2\mu\mu' \cos \Delta_{\phi} \end{pmatrix} \quad (21)$$

with  $K_{\pm}(\mu) = 1 \pm \mu^2$ ,  $\Delta_{\phi} = 2(\phi' - \phi)$ . The particular form of the metric tensor makes  $\iota$  still dependent on  $\phi$  in spite of the choice of a special reference system. However, this dependence is not too cumbersome. In fact, it is

possible to introduce a change of variables [24] to eliminate the dependence on the azimuthal angle. The new quantities,  $\tilde{I}$ ,  $\tilde{Q}$  and  $\tilde{U}$  are related to the old ones by the following relation:

$$\begin{cases} I(\mu, \phi) = \tilde{I}_\pm(\mu)(1 - \mu^2) \cos 2\phi + \tilde{I}_\times(\mu)(1 - \mu^2) \sin 2\phi \\ Q(\mu, \phi) = \tilde{Q}_\pm(\mu)(1 + \mu^2) \cos 2\phi + \tilde{Q}_\times(\mu)(1 + \mu^2) \sin 2\phi \\ U(\mu, \phi) = -\tilde{U}_+ 2\mu \sin 2\phi + \tilde{U}_\times 2\mu \cos 2\phi \end{cases} \quad (22)$$

It is easy to prove that, with these new variables, only  $\hat{P}^2$  provides a non vanishing contribution to the integral of equation (7) over  $\phi$ . This is why we have considered only this term in equation (21). Also, as the Boltzmann equation becomes independent of  $\phi$ , we can still develop fluctuations of  $\tilde{I}, \tilde{Q}$  and  $\tilde{U}$  in Legendre polynomials. Thus, equation (20) becomes:

$$\begin{cases} \dot{\tilde{t}}_\epsilon + \frac{ik\mu}{a} \tilde{t}_\epsilon - 2\dot{h}_\epsilon = -\sigma_T n_e (\tilde{t}_\epsilon + \Psi) \\ \dot{\tilde{q}}_\epsilon + \frac{ik\mu}{a} \tilde{q}_\epsilon = -\sigma_T n_e (\tilde{q}_\epsilon - \Psi) \\ \tilde{q}_\epsilon + \tilde{u}_\epsilon = 0 \end{cases} \quad (23)$$

where

$$\Psi = 3/5\tilde{\eta}_{\epsilon,0} + 6/35\tilde{\eta}_{\epsilon,2} + 1/210\tilde{\eta}_{\epsilon,4} - 1/10\tilde{\sigma}_{\epsilon,0} + 1/35\tilde{\sigma}_{\epsilon,2} - 1/210\tilde{\sigma}_{\epsilon,a} \quad (24)$$

and  $\epsilon$  identifies either the + or the  $\times$  polarization state of the gravitational wave.

### 3.3. NUMERICAL CALCULATIONS

We restrict ourselves to a Universe composed by baryons, cold dark matter, photons and three families of massless neutrinos. The equations describing anisotropy and polarization of the CMB have been written above. In Fourier space, the equations describing fractional fluctuations in the remaining cosmic components are [42,43,44]:

$$\frac{\partial t_\nu}{\partial t} + i\frac{k\mu}{a} t_\nu = y \quad (25)$$

$$\ddot{h} + 2\frac{\dot{a}}{a}\dot{h} = 8\pi G (\rho_B \delta_B + \rho_{CDM} \delta_{CDM} + 2\rho_\gamma \delta_\gamma + 2\rho_\nu \delta_\nu) \quad (26)$$

$$\dot{h}_{33} - \dot{h} = \frac{16\pi G a}{k} (\rho_B v + \rho_\gamma f_\gamma + \rho_\nu f_\nu) \quad (27)$$

$$\dot{\delta}_B = \frac{\dot{h}}{2} - i\frac{kv}{a} \quad (28)$$



$$\dot{v}_b + H(t)v_b = \sigma_T n_e \left( f_\gamma - \frac{4}{3}v_b \right) \quad (29)$$

$$\dot{\delta}_{CDM} = \frac{\dot{h}}{2} \quad (30)$$

and

$$\ddot{h}_{+, \times} + 3\frac{\dot{a}}{a}\dot{h}_{+, \times} + \frac{k^2}{a^2}h_{+, \times} = 0 \quad (31)$$

for scalar and tensor fluctuations, respectively.

Eq.(25) describes the fluctuations in the massless neutrinos. We follow this component only when the perturbation proper wavelength is larger than one tenth of the horizon. Afterwards, free streaming rapidly damps fluctuations in this hot component.

The time evolution of the baryon and CDM density contrasts and of the baryon peculiar velocity are described by Eq.(28), (30) and (29) respectively. The system for the scalar fluctuations is closed by Eq.(26) and (27) describing the field equations for the trace and the 3 – 3 component of the metric perturbation tensor, while Eq.(31) is all we need to describe the evolution of the metric perturbations for tensor fluctuations. We numerically integrate the previous equations from redshift  $z = 10^7$  up to the present. The abundance of free electrons,  $n_e$ , is evaluated following a standard recombination scheme [45,46] for  $H$  and  $^4He$ , taken in the ratio 77 : 33. In the following we also consider the possibility that the universe reionized instantaneously at redshift  $z_{rh} \ll 1000$ , and remained completely reionized up to the present.

#### 4. Computing the Correlation Function for Anisotropy and Polarization

Under the assumption of gaussian initial conditions, the statistical properties of the CMB anisotropy and polarization patterns are fully described in terms of their correlation functions. The stochastic anisotropic component of the CMB is conveniently expanded in spherical harmonics:  $\delta T(\hat{\gamma})/T_0 = \sum_{lm} a_{lm} Y_m^l(\hat{\gamma})$ . The coefficients  $a_{lm}$  are random gaussian variables with zero mean and rotationally invariant variances,  $C_\ell \equiv \langle |a_{lm}|^2 \rangle$ . The mean (over the ensemble) correlation function of the anisotropy pattern has the standard expression:

$$\left\langle \frac{\delta T(\vec{\gamma}_1)}{T_0} \frac{\delta T(\vec{\gamma}_2)}{T_0} \right\rangle = \frac{1}{4\pi} \sum_{\ell} (2\ell + 1) C_\ell P_\ell(\cos \theta) \quad (32)$$

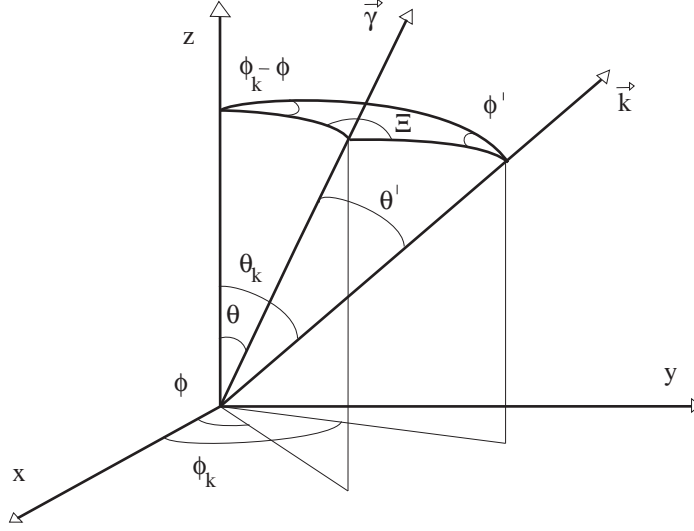


Figure 3. Laboratory reference system.

where  $\cos \theta = \vec{\gamma}_1 \cdot \vec{\gamma}_2$ , and

$$C_\ell = \frac{A_S}{8\pi} \int_0^\infty \frac{|\sigma_\ell(k)|^2}{(2\ell+1)^2} k^{n_S+2} dk \quad (33)$$

Here the primordial power spectrum of scalar fluctuations is assumed to have the standard form  $P(k) = A_S k^{n_S}$ . In the case of tensor fluctuations, the change of variables needed to achieve rotationally symmetry [see equation (22)] must be taken into account. Then, the correlation function of the CMB anisotropy induced by tensor modes reads:

$$\left\langle \frac{\delta T(\vec{\gamma}_1)}{T_0} \frac{\delta T(\vec{\gamma}_2)}{T_0} \right\rangle = \frac{A_T}{128\pi^3} \int \sum_{\ell_1 \ell_2} \Pi_{\ell_1, \ell_2}(k, \vec{\gamma}'_1, \vec{\gamma}'_2) P_{\ell_1}(\mu'_1) P_{\ell_2}(\mu'_2) k^{n_T-3} d^3 k \quad (34)$$

where

$$\Pi_{\ell_1, \ell_2} = K_-(\mu'_1) K_-(\mu'_2) [\tilde{\sigma}_{\ell_1}^\times \tilde{\sigma}_{\ell_2}^{\times*} \cos(2\phi'_1) \cos(2\phi'_2) + \tilde{\sigma}_{\ell_1}^+ \tilde{\sigma}_{\ell_2}^{+*} \sin(2\phi'_1) \sin(2\phi'_2)] \quad (35)$$

where the power spectrum of metric fluctuations due to tensor modes is assumed to be  $\tilde{P}(k) = A_T k^{n_T-3}$ . Assuming  $\tilde{\sigma}_\ell^+ = \tilde{\sigma}_\ell^\times$  and making some algebraic manipulations yield:

$$\left\langle \frac{\delta T(\vec{\gamma}_1)}{T_0} \frac{\delta T(\vec{\gamma}_2)}{T_0} \right\rangle = \frac{A_T}{128\pi^3} \int \sum_{\ell_1 \ell_2} \Upsilon(\vec{\gamma}'_1, \vec{\gamma}'_2) \tilde{\sigma}_{\ell_1}^+ \tilde{\sigma}_{\ell_2}^{+*} P_{\ell_1}(\mu'_1) P_{\ell_2}(\mu'_2) k^{n_T-3} d^3 k \quad (36)$$

where

$$\Upsilon = [2(\vec{\gamma}_1 \cdot \vec{\gamma}_2 - \mu'_1 \mu'_2)^2 - K_-(\mu'_1) K_-(\mu'_2)] \quad (37)$$

and, finally [47,48,49],

$$\left\langle \frac{\delta T(\vec{\gamma}_1)}{T_0} \frac{\delta T(\vec{\gamma}_2)}{T_0} \right\rangle = \frac{1}{4\pi} \sum_{\ell} (2\ell + 1) \tilde{C}_{\ell} P_{\ell}(\cos \theta) \quad (38)$$

with

$$\tilde{C}_{\ell} = \frac{A_T}{8\pi} \frac{(\ell + 2)!}{(\ell - 2)!} \int_0^{\infty} \frac{|\tilde{\Sigma}_{\ell}(k)|^2}{(2\ell + 1)^2} k^{n_T-1} dk \quad (39)$$

and

$$\tilde{\Sigma}_{\ell}(k) = \frac{\tilde{\sigma}_{\ell-2}^+}{(2\ell - 1)(2\ell - 3)} - 2 \frac{\tilde{\sigma}_{\ell}^+}{(2\ell - 1)(2\ell + 3)} + \frac{\tilde{\sigma}_{\ell+2}^+}{(2\ell + 5)(2\ell + 3)} \quad (40)$$

As discussed in Section 2, the  $Q$  and  $U$  Stokes parameters vary because of a clockwise rotation  $\Xi$  of the reference system in the polarization plane :

$$\begin{cases} Q_{\Xi} = Q \cos(2\Xi) + U \sin(2\Xi) \\ U_{\Xi} = -Q \sin(2\Xi) + U \cos(2\Xi) \end{cases} \quad (41)$$

So, the perturbations to  $Q$  and  $U$  in the Lab frame are related with those in  $\vec{k}$  space by the following relation:

$$\frac{Q(\vec{x}, \theta, \phi)}{T_0} = \frac{1}{32\pi^3} \int q(\vec{k}) e^{i\vec{k}\vec{x}} \cos[2\Xi(\vec{k})] d^3 k \quad (42)$$

$$\frac{U(\vec{x}, \theta, \phi)}{T_0} = \frac{-1}{32\pi^3} \int q(\vec{k}) e^{i\vec{k}\vec{x}} \sin[2\Xi(\vec{k})] d^3 k \quad (43)$$

The correlation function for the  $Q$  parameter for scalar modes can be written as follows:

$$\left\langle \frac{Q(\vec{\gamma}_1)}{T_0} \frac{Q(\vec{\gamma}_2)}{T_0} \right\rangle = \frac{A_S}{128\pi^3} \int \sum_{\ell_1, \ell_2} \eta_{\ell_1}^* \eta_{\ell_2} \cos(2\Xi_1) \cos(2\Xi_2) P_{\ell_1}(\mu'_1) P_{\ell_2}(\mu'_2) k^{n_S} d^3 k \quad (44)$$

The correlation function for  $U$  has a similar expression with  $\cos 2\Xi \rightarrow \sin 2\Xi$ . Let us identify the line of sight  $\vec{\gamma}_1$  with the  $z$ -axis of the Lab frame. In this case,  $(\theta_1, \phi_1) = (0, 0)$ ,  $\theta'_1 = \theta_k$  and  $\phi'_1 = -\phi_k$  (see Figure 3). In the small angle approximation,  $\cos(2\Xi_1) \sim \cos(2\Xi_2) \sim \cos(2\phi_k)$ , and equation (44) yields :

$$\left\langle \frac{Q(\vec{z})}{T_0} \frac{Q(\vec{\gamma}_2)}{T_0} \right\rangle = A(\theta) + B(\theta, \phi) \quad (45)$$

where

$$A(\theta) = \frac{A_S}{256\pi^3} \int \sum_{\ell_1 \ell_2} \eta_{\ell_2}(k) \eta_{\ell_1}^*(k) P_{\ell_1}(\mu'_k) P_{\ell_2}(\mu'_2) k^{n_S} d^3k \quad (46)$$

and

$$B(\theta, \phi) = \frac{A_S}{256\pi^3} \int \sum_{\ell_1 \ell_2} \eta_{\ell_2}(k) \eta_{\ell_1}^*(k) P_{\ell_1}(\mu'_k) P_{\ell_2}(\mu'_2) \cos(4\phi_k) k^{n_S} d^3k \quad (47)$$

The first term has the standard expression :

$$A(\theta) = \frac{1}{4\pi} \sum_{\ell} (2\ell + 1) C_{\ell}^Q P_{\ell}(\cos \theta) \quad (48)$$

with

$$C_{\ell}^Q = \frac{A_S}{16\pi} \int_0^{\infty} \frac{|\eta_{\ell}(k)|^2}{(2\ell + 1)^2} k^{n_S+2} dk \quad (49)$$

For the second term, we can develop  $P_{\ell_1}(\cos \theta_k)$  in associated Legendre polynomials with  $m = 4$ :

$$P_{\ell_1}(\cos(\theta_k)) = \sum_{\ell' \geq 4}^{\infty} \alpha_{\ell_1, \ell'} P_{\ell'}^4(\cos(\theta_k)) \quad (50)$$

where

$$\alpha_{\ell_1 \ell'} = \frac{2\ell' + 1}{2} \frac{(\ell' - 4)!}{(\ell' + 4)!} A_{\ell_1, \ell'} \quad (51)$$

and  $A_{\ell_1, \ell'} = \int_{-1}^1 P_{\ell_1} P_{\ell'}^4 d(\cos \theta_k)$  has the following values :

$$\begin{cases} A_{\ell, \ell} = \frac{2}{2\ell+1} \frac{\ell!}{(\ell-4)!} & \ell' \equiv \ell \\ A_{\ell, \ell'} = 8(\ell'^2 + \ell' - 3(\ell^2 + \ell + 2)) & \ell' = \ell + 2, \ell + 4, \dots, \ell + 2n \\ A_{\ell, \ell'} = 0 & \ell' = \ell + 1, \ell + 3, \dots, \ell + 2n + 1 \\ A_{\ell, \ell'} = 0 & \ell' < \ell \end{cases} \quad (52)$$

From the definition of the spherical harmonics it also follows:

$$P_{\ell'}^4(\cos \theta_k) \cdot \cos(4\phi_k) = \frac{1}{2} \sqrt{\frac{4\pi}{2\ell'+1} \frac{(\ell'+4)!}{(\ell'-4)!}} (Y_{\ell'}^4(\vec{k}) + Y_{\ell'}^{-4}(\vec{k})) \quad (53)$$

Now, execute the following steps:

1. Insert the (50) in the (47)
2. Develop the product between the Legendre polynomial and the cosine with the (53)
3. Integrate in  $d\Omega_k$
4. Use again the (53) to transform the spherical harmonics in  $P_{\ell'}^4$
5. Develop the  $P_{\ell'}^4$  in  $P_{\ell}$ .

At the end, in the small angle approximation, it is possible to write [29,50,71]:

$$\left\langle \frac{Q(\vec{z})}{T_0} \frac{Q(\vec{\gamma}_2)}{T_0} \right\rangle = \frac{1}{4\pi} \sum_{\ell} (2\ell+1) (C_{\ell}^Q + \cos(4\phi) B_{\ell}) P_{\ell}(\cos \theta) \quad (54)$$

where the two terms  $C_{\ell}^Q$  and  $B_{\ell}$  are defined, for scalar perturbations, as follows:

$$C_{\ell}^Q = \frac{A_S}{16\pi} \int \frac{|\eta_{\ell}|^2}{(2\ell+1)^2} k^{n_S+2} dk \quad (55)$$

$$B_{\ell} = \frac{A_S}{64\pi} \sum_{\ell_1 \ell_2} \frac{(\ell_2-4)!}{(\ell_2+4)!} A_{\ell, \ell_2} A_{\ell_1, \ell_2} \int \eta_{\ell_1}^* \eta_{\ell_2} k^{n_S+2} dk \quad (56)$$

For tensor fluctuations, the calculation is similar. The final result is [30,50,71]:

$$\left\langle \frac{Q(\vec{z})}{T_0} \frac{Q(\vec{\gamma}_2)}{T_0} \right\rangle = \frac{1}{4\pi} \sum_{\ell} (2\ell+1) (\tilde{C}_{\ell}^Q + \cos(4\phi) \tilde{B}_{\ell}) P_{\ell}(\cos \theta) \quad (57)$$

where

$$\tilde{C}_{\ell}^Q = \frac{A_T}{16\pi} \int \frac{(|T_{\ell}|^2 + 4|R_{\ell}|^2)}{(2\ell+1)^2} k^{n_T-1} dk, \quad (58)$$

$$\tilde{B}_{\ell} = \frac{A_T}{64\pi} \sum_{\ell_1 \ell_2} \frac{(\ell_2-4)!}{(\ell_2+4)!} A_{\ell, \ell_2} A_{\ell_1, \ell_2} \int (T_{\ell_1}^* T_{\ell_2} + 4R_{\ell_1}^* R_{\ell_2}) k^{n_T-1} dk, \quad (59)$$

$$R_{\ell} = \frac{\ell+1}{2\ell+3} \tilde{\eta}_{\ell+1}^+ + \frac{\ell}{2\ell-1} \tilde{\eta}_{\ell-1}^+, \quad (60)$$

$$T_\ell = \frac{(\ell+2)(\ell+1)}{(2\ell+3)(2\ell+5)} \tilde{\eta}_{\ell+2}^+ + 2 \frac{6\ell^3 + 9\ell^2 - \ell - 2}{(2\ell+3)(2\ell-1)(2\ell+1)} \tilde{\eta}_\ell^+ + \frac{\ell(\ell-1)}{(2\ell-1)(2\ell-3)} \tilde{\eta}_{\ell-2}^+, \quad (61)$$

and  $A_{\ell_1, \ell_2} = \int P_{\ell_1}(x) P_{\ell_2}^4(x) dx$ .

An interesting case is the correlation function between CMB anisotropy and polarization. For scalar fluctuations and in the small angle approximation, the result is [29,50,71]:

$$\left\langle \frac{\delta T(\vec{z})}{T_0} \frac{Q(\vec{\gamma}_2)}{T_0} \right\rangle = \frac{1}{4\pi} \sum_\ell (2\ell+1) C_\ell^{QT} \cos(2\phi) P_\ell^2(\cos\theta) \quad (62)$$

where

$$C_\ell^{QT} = \frac{A_S}{16\pi} \sum_{\ell_1} \frac{(\ell-2)!}{(\ell+2)!} B_{\ell_1, \ell} \int \frac{\sigma_{\ell_1}^* \eta_\ell}{(2\ell+1)} k^{n_S+2} dk \quad (63)$$

and the integral  $B_{\ell_1, \ell_2} = \int P_{\ell_1}(x) P_{\ell_2}^2(x) dx$  has the values :

$$\begin{cases} B_{\ell, \ell} = -\frac{2}{2\ell+1} \frac{\ell!}{(\ell-2)!} & \ell' = \ell \\ B_{\ell, \ell'} = 4 & \ell' = \ell+2, \ell+4, \dots, \ell+2n \\ B_{\ell, \ell'} = 0 & \ell' = \ell+1, \ell+3, \dots, \ell+2n+1 \\ B_{\ell, \ell'} = 0 & \ell' < \ell \end{cases} \quad (64)$$

## 5. Numerical Results and Discussion

With the formalism developed in the previous Sections, we are now able to make theoretical predictions for CMB anisotropy and polarization. As stated before, we restrict ourselves to the Cold Dark Matter scenario. This is not quite enough to completely define the model, as we have to deal with quite a number of parameters. We have to fix : i) the total density parameter,  $\Omega_0$ , and the cosmological constant,  $\Lambda$ ; ii) the baryonic abundance,  $\Omega_b$ ; iii) the Hubble constant; iv) the primordial spectral index for spectral fluctuations; v) the relative amplitude of scalar and tensor fluctuations; vi) the spectral index for tensor fluctuations; vii) the thermal history of the universe; viii) the overall amplitude for scalar fluctuations.

The baryonic abundance is quite severely restricted by primordial nucleosynthesis. We consider the fiducial value of  $\Omega_b = 0.05 \pm 0.02$  as representative of the possible uncertainty in this parameter. We remind that changes in  $\Omega_b$  yield variations in the pressure of the photon-baryon fluid before recombination, and then variations in the amplitude of the first acoustic peak in the anisotropy power spectrum.

For flat models the value of the Hubble constant is usually taken to be  $H_0 = 50 \text{Kms}^{-1}/\text{Mpc}$  for age considerations, even if the estimated globular cluster age allows for slightly different values:  $40 \text{Kms}^{-1}/\text{Mpc} < H_0 < 65 \text{Kms}^{-1}/\text{Mpc}$  [63]. Small variations in the Hubble constant yield huge variations in the radiation power spectrum, modifying both the amplitudes and positions of the acoustic peaks.

The primordial index for scalar fluctuations,  $n_S$ , is usually taken to be unity, as inflation suggests. However, in more general inflationary scenarios,  $n_S$  can be either smaller or larger than unity [64]. This modifies the relative power between the anisotropy on small and large angular scale. Power-law inflationary models predict  $n_S < 1$ , but also a background of gravitational waves. A standard prediction is that the ratio of the quadrupoles induced by scalar and tensor fluctuations is:

$$\frac{\tilde{C}_2}{C_2} = -7n_T \sim 7(1 - n_s), \quad (65)$$

which allows to relate amplitudes and shapes of primordial power spectra for scalar and tensor fluctuations, respectively [18,49,64].

The thermal history of the universe, in its standard form, assumes recombination of the primordial plasma at redshift  $\sim 1000$ . However, both the Gunn-Peterson test [65] and the enriched composition of the intracluster medium [74,75] suggest the possibility of a considerable energy release during the early stages of galaxy formation and evolution.

Finally, the amplitude of fluctuations it is still unknown from first principles, and it is fixed in order to match the observed rms temperature fluctuations ( $29 \pm 1 \mu\text{K}$ ) of the COBE/DMR anisotropy maps [53].

In Figure 4 we show theoretical predictions for CMB anisotropy and polarization of a standard Cold Dark Matter Model with  $\Omega_0 = 1$ ,  $\Omega_b = 0.05$ ,  $H_0 = 50 \text{Kms}^{-1}/\text{Mpc}$ ,  $n_S = 1$  and standard recombination. The anisotropy power spectrum for scalar fluctuations has a flat behavior at low  $\ell$ 's, where the Sachs-Wolfe effect [66] dominates, and a structure of peaks at higher  $\ell$ 's, defined by the acoustic oscillations in the photon-baryon fluid experienced before recombination by fluctuations smaller than the acoustic horizon. The damping at high  $\ell$ 's is due to the finite thickness of the last-scattering surface [67]. The first peak at  $\ell \sim 200$  corresponds to fluctuations that entered the horizon at recombination, which subtends an angle  $\sim 2^\circ h^{-1}$ . The polarization power spectrum has instead power only at  $\ell > 200$ , *i.e.* on scales  $< 2^\circ h^{-1}$ . The case of pure tensor fluctuations is show in Figure 4 only for the didactic purposes. In this case, the anisotropy spectrum has power only at  $\ell < 200$  and the polarization spectrum shows a prominent peak at  $\ell \sim 100$ . Note that the polarization spectrum has an amplitude

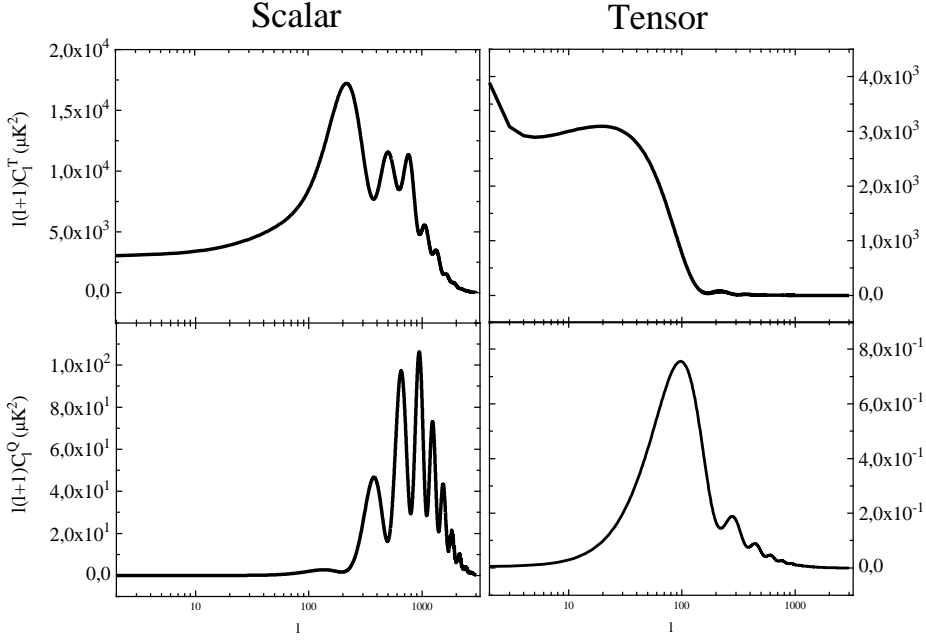


Figure 4. Anisotropy (top) and polarization (bottom) power spectrum for scalar (left) and tensor (right) fluctuations. Each model is normalized to COBE  $\sigma(10^\circ) = 29\mu K$ .

lower than the anisotropy spectrum by a factor  $\sim 10^2$  and  $\sim 10^4$  for scalar and tensor fluctuations, respectively.

Real experiments are sensitive to a limited region of the power spectrum, because of the antenna beam and modulation techniques. For anisotropy experiments, this effect can be parameterized by a window function,  $W_\ell$ , so that the variance of temperature fluctuations detected by an experiment can be written as:

$$\left\langle \left( \frac{\delta T(\vec{\gamma})}{T_0} \right)^2 \right\rangle = \frac{1}{4\pi} \sum_{\ell} (2\ell + 1) C_{\ell} W_{\ell} \quad (66)$$

A similar expression holds for the variance of the fluctuations of the  $Q$  parameter:

$$\left\langle \left( \frac{Q(\vec{\gamma})}{T_0} \right)^2 \right\rangle = \frac{1}{4\pi} \sum_{\ell} (2\ell + 1) C_{\ell}^Q W_{\ell} \quad (67)$$



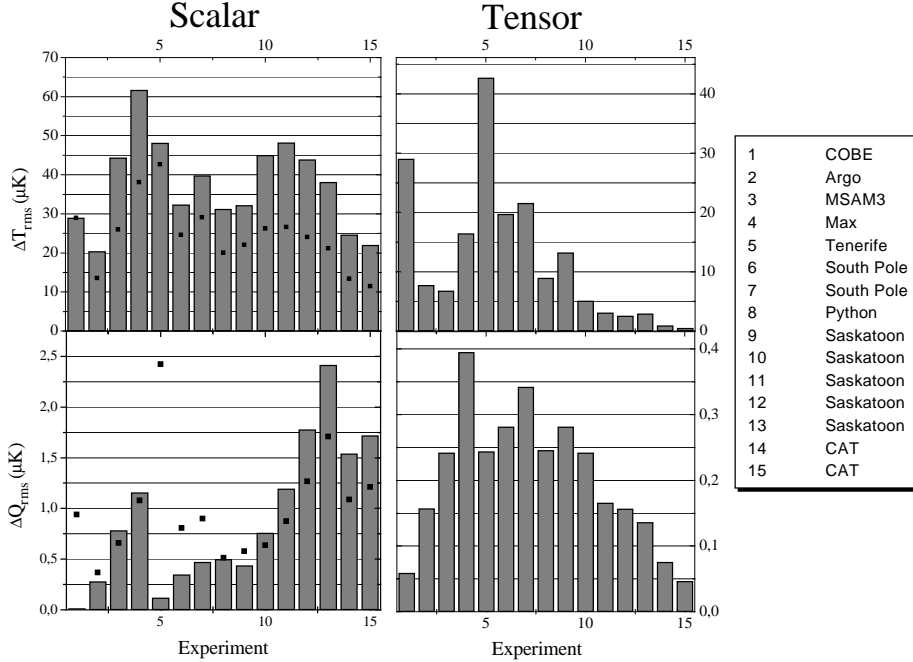


Figure 5. R.m.s. values for anisotropies (top) and polarization (bottom) scheduled for scalar (left) and tensor (right) models for different experiments [53...61]. The tensor model has  $n_T = 0$  and the scalar model has  $n_S = 1$ . Each model is normalized to COBE  $\sigma(10^\circ) = 29\mu K$ . The dot of the left side represents the values for a scalar reionized model at  $z_r \sim 70$ .

In fact, it can be proved that the azimuthal contribution [see equations (54) and (57)] to the  $Q$  variance vanishes. In equation (67) we use the same anisotropy window functions, in order to give an order of magnitude estimate of the level of measurable polarization at different angular scales.

In Figure 5 we plot the expected rms values for CMB anisotropy and polarization using 15 different window functions corresponding to 9 different anisotropy experiments. The level of polarization from scalar modes is below the current experimental sensitivity, even for small scale experiments such as Saskatoon or CAT that are sensitive to multipole  $\ell \sim 400$  where the polarization has the first two peaks. The rms level from pure tensor modes, even for the MAX experiment that seems to have the best window function, is below  $0.5 \mu K$ , so the separation between scalar and tensor fluctuations do not seem to be at hand with polarization measurements [25,26,27,28,73]. This can be done by combining anisotropy measurements at both large (where tensor modes could contribute) and small

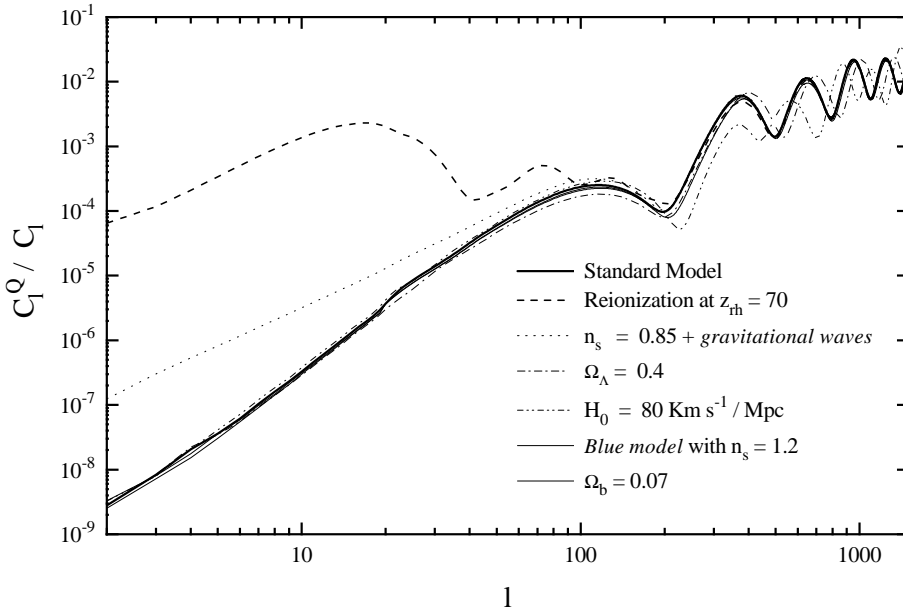


Figure 6. Dependence of polarization on cosmological parameters.

(where tensor modes do not contribute) angular scales [49,72,73]. An accurate mapping of the anisotropy pattern with both high sensitivity and high angular resolution will be provided by planned, dedicated space missions such as COBRAS/SAMBA [68] and MAP [52]. At the moment the bulk of degree-scale detections, combined with the COBE/DMR and Tenerife experiments, seems to suggest a spectral index for scalar fluctuations  $n_S \geq 1$  [69] and a negligible contribution of tensor modes.

As mentioned above, there are several free parameters, each with its own uncertainty, which define a theoretical model. So, it is interesting to explore the sensitivity of the polarization level relative to the anisotropy one. To show this, we plot in Figure 6 the quantity  $C_\ell^Q/C_\ell$  as a function of  $\ell$ , for different choices of the model parameters. Generally speaking the effects of the variation of these parameters on anisotropy and polarization are similar: both quantities tend to decrease with increasing  $H_0$  and tend to increase when a cosmological constant  $\Omega_\Lambda = 1 - \Omega_0$  is taken into account. In particular, varying  $n_S$  or  $\Omega_b$  yields basically no variations on the  $C_\ell^Q/C_\ell$  ratio. Moreover, decreasing the spectral index and adding gravitational waves increase the large scale polarization, but, as we have shown,

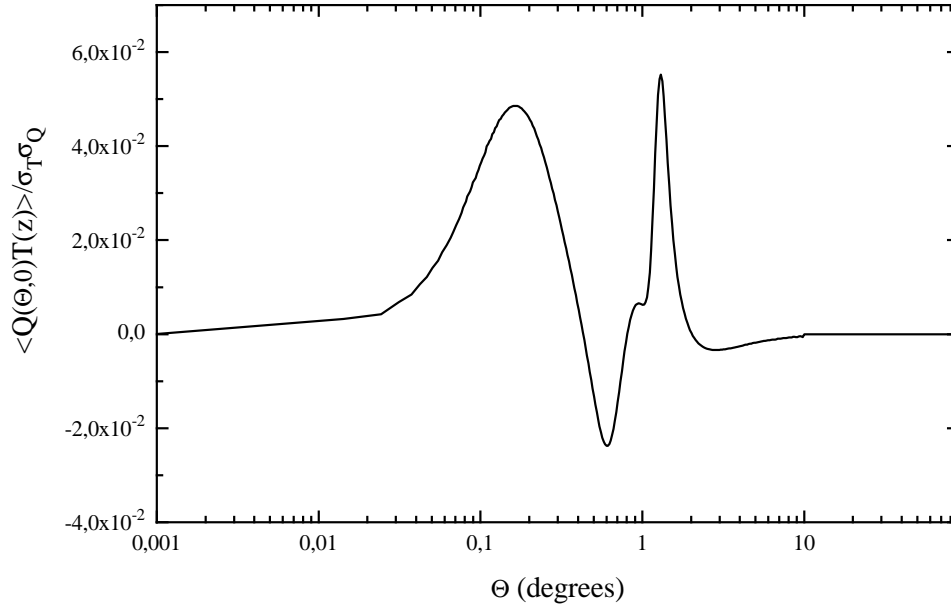


Figure 7. Polarization - Anisotropy correlation function.

not enough to pass the threshold of present day detector sensitivity. So, even taking into account reasonable uncertainties in the parameters, it seems that only with an huge increment in the experimental sensitivity (see the accompanying paper by F. Melchiorri et al. in this volume) and/or a space mission [52,70,71] a robust detection of the polarization spectrum over a wide range of  $\ell$ 's would be possible. Coulson et al. [29] suggested searching a correlation between the temperature in one direction and the polarization in a circle at distance  $\Theta$  from that direction. The shape of the correlation function (62) measurable in this way is show in Figure 7. As we can see the cross correlation is positive on scales  $> 1^\circ$ , negative on scales between  $0.5^\circ$  and  $1^\circ$  and positive again on scales  $< 0.5^\circ$ . According to [52] the future MAP satellite would have the capability to measure the expected amplitude of this signal.

The final item to be investigated is the dependence of CMB anisotropy and polarization on the thermal history of the universe. A reionization at  $z \leq 100$  produces a new, later and thicker last scattering surface. The effect of such a new last scattering surface is to smooth the anisotropy on small angular scales and to leave unchanged the level of anisotropy on large

angular scales. The effect of reionization on polarization is to reduce the polarization on small scales but to increase the polarization level at large angular scales. This is shown again in Figure 6. Thus, possible detection of polarization between  $1^\circ$  and  $10^\circ$ , say, would be an evidence for an early re-heating of the intergalactic medium.

## 6. Conclusions

Numerical solutions of the Boltzmann transport equation show that a certain degree of polarization must be present as a consequence of the primordial fluctuations responsible for the structure formation. The level of polarization depends strongly on the angular scale, much more than in the case of anisotropy, quite independently of the choice of the model parameters. At angular scales larger than one degree we do not expect detectable polarization unless the universe was reionized at early times  $z \geq 40$ . At small angular scales the polarization may reach the 5 – 10% of the anisotropy. However, a polarization of a few percent at angular scales of  $1^\circ$ - $10^\circ$  could be explained only because reionization: a search for polarization at these scale is therefore important in the study of the thermal history of the universe. Also, it seems hard to disentangle tensor from scalar perturbations through measurements of polarization, due to the tenuity of the signal.

## 7. Acknowledgments

We would like to thank Paolo de Bernardis for comments and suggestions. AM thanks Arthur Kosowsky for helpful discussions. This work has been supported by MURST.

## References

1. Rees M. J., (1968) Polarization and Spectrum of the Primeval Radiation in an Anisotropic Universe, *Astr. J. Lett.*, **153**, L1
2. Caderni N., Fabbri R., Melchiorri B., Melchiorri F., Natale V., (1978) Polarization of the Microwave Background Radiation I: Theory, *Phys. Rev. D*, **17**
3. Dautcourt G., Rose K., (1978), *Astron. Nachrichten*, **299**, 13
4. Basko M.M., Polnarev A.G., (1980), *Sov. Astron.*, **24**, 268
5. Negroponte, Silk J., (1980), *Phys. Rev. Lett.*, **44**, 1433
6. Tolman B.W., Matzner R.A., (1984), *Proc. R. Soc. Lond.*, **391**, A392
7. Fabbri R. Milaneschi E., (1985) , *A&A*, **151**, 714
8. Milaneschi E. Fabbri R., (1986) , *A&A*, **162**, 6
9. Fabbri R., Tamburrano, (1987) , *A&A*, **179**, 11F
10. Kaiser N., (1983), *Mont. No. R. Astr. Soc.*, **101**, 1169
11. Bond J. R., Efstathiou G., (1984), *Ap. J.*, **285**, L45
12. Bond J. R., Efstathiou G., (1987), *Mon. No. R. Astr. Soc.*, **226**, 655
13. Milaneschi E., Valdarnini R., (1986), *A&A*, **162**, 5-12
14. Ceccarelli C., Dall'Oglio G., de Bernardis P., Masi S., Melchiorri B., Melchiorri F., Moreno G., Pietranera L., Pucacco G., (1982), The Polarization of the Cosmic

- Background and the Universal Magnetic Field, *The Birth of the Universe* Eds. J. Audouze, J. Tran Thanh Van, Edition Frontieres, 191
15. Efstathiou G., (1988), *Large Scale motions in the Universe: a vatican study week. Edited by Vera C. Rubin George V. Coyne*, Princeton series in physics
  16. Smoot G. et al., (1992), *Ap. J.*, **396**, L1
  17. Krauss L.M., White M., (1992), *Phys. Rev. Lett.*, **69**, 869-872
  18. Davis R.L. et al., (1992), *Phys. Rev. Lett.*, **69**, 1856
  19. Liddle A.R., Lyth D., (1992), *Phys. Lett.*, **B 291**, 391
  20. Lidsey J.E. Coles P., (1992), *Mon. Not. R. Astr. Soc.*, **358**, 57
  21. Salopek D., (1992), *Phys. Rev. Lett.*, **69**, 3602
  22. Lucchin F., Matarrese S., Mollerach S., (1992), *Ap. J.*, **401**, L49
  23. Sourdeep T. et al., (1992), *Phys. Lett.*, **A 7**, 3541
  24. Polnarev, A.G., (1985), *Sov. Astr.*, **29**, 607
  25. Crittenden R., Davis R.L., Steinhardt P.J., (1993), *Ap. J.*, **417**, L13
  26. Frewin R.A., Polnarev A.G., Coles P. , (1994), *Mon. No. R. Astr. Soc.*, **266**, L21
  27. Sazhin M.V., Benitez N., (1995), *Astro. Lett. and Communications*, **32**, 105
  28. Ng K.L., Ng K.W., (1995), *Ap. J.*, **445**, 521
  29. Coulson D., Crittenden R., Turok N.G. , (1994), *Phys. Rev. Lett.*, **73**, 2390
  30. Crittenden R., Coulson D., Turok, N.G. , (1995), *Phys. Rev. D*, **52**, 5402
  31. Hu W., Scott D., Sugiyama N., White M., (1995), *Phys. Rev. D*, **52**, 5498
  32. Chun-Pei M., Bertschinger E., (1995), *Apj*, **455**, 7
  33. Kosowsky A., Loeb A. , (1996), *Apj*, in press
  34. Penzias A.A., Wilson R.W., (1965) *Ap.J.*, **142**, 419
  35. Nanos G.P., (1979) , *Ap. J.*, **232**, 341
  36. Caderni N., Fabbri R., Melchiorri B., Melchiorri F., Natale V., (1978) Polarization of the Microwave Background Radiation I: an Infrared Survey of the Sky, *Phys. Rev. D*, **17**
  37. Lubin P., Smoot G., (1981) , *Ap. J.*, **273**, L51
  38. Wollack et al, (1993), *Ap. J.*, **419**, L49
  39. Chandrasekhar, S., (1960), *Radiation Transfer*, Ed. Dover
  40. Peebles P.J.E., Yu J.T., (1970), *Ap. J.*, **162**, 815
  41. Peebles P.J.E., (1980), The large scale structure of the Universe.
  42. Peebles P.J.E, (1981), *Ap. J.*, **243**, L119
  43. Peebles P.J.E., (1982), *Ap. J.*, **258**, 415
  44. Peebles P.J.E., (1982), *Ap. J.*, **263**, L1
  45. Peebles P.J.E., (1968), *Ap. J.*, **153**, 1
  46. Jones B.J., Wyse R., (1985), *A & A*, **149**, 144-150
  47. Fabbri R., Pollock M., (1983), *Phys. Letters*, **125B**, 445
  48. Abbot L.F., Wise M., (1984), *Nucl. Phys.*, **B244**, 541
  49. Crittenden R., Bond J.R., Davis R.L., Efstathiou G., Steinhardt P., (1993), *Phys. Rev Lett.*, **71**, 324c
  50. Kosowsky A., (1996), *Annals of Physics*, **246**, 49
  51. Steinhardt P., (1995), *Astro-ph 9502024*
  52. Bennett C.L. et al., (1995), MAP MIDEX mission proposal.
  53. Bennett C.L. et al., (1996), *Ap. J.*, **464**, L1
  54. Hancock S. et al, (1994), *Nature*, **367**, 333
  55. Gundersen J.O. et al., (1993), *Ap. J.*, **413**, L1
  56. Dragovan M. et al., (1993), *Ap. J.*, **427**, L67
  57. de Bernardis P. et al., (1994), *Ap. J.*, **422**, L33
  58. Tanaka S.T. et al., (1996), *Ap. J.*, in press
  59. Cheng E.S. et al., (1994), *Ap. J.*, **422**, L40
  60. Netterfield et al., (1996), *Astro-ph 9601197*
  61. Scott P.F. et al., (1996), *Ap. J.*, **461**, L1
  62. Jackson J.D., (1962), *Classical electrodynamics*, John Wiley, NY
  63. Kolb E.W. Turner M.S., (1993), *The Early Universe*, Addison Wesley, CA

64. Kolb E.W. Vadas S.L., (1994), *Phys. Rev. D*, **50**, 4, 2479
65. Gunn J.E. Peterson B.A., (1965), *Ap. J.*, **142**, 1633
66. Sachs R.K. Wolfe A.M., (1967), *Ap. J.*, **147**, 73
67. Silk J., (1968), *Ap. J.*, **151**, 459
68. Bersanelli M. et al., (1996), *COBRAS/SAMBA proposal*, D/SCI(96)3
69. de Bernardis P., Balbi A., de Gasperis G., Melchiorri A., Vittorio N., (1996), *Astro-ph 9609154*.
70. Kamionkowski M., Kosowsky A., Stebbins A., (1996), *Astro-ph 9609132*
71. Seljak U., (1996), *Astro-ph 9608131*
72. Knox L. Turner M.S., (1994), *Phys. rev. Lett.*, **73**
73. Turner M.S., (1996), *Astro-ph 9607066*
74. Mushotzky R.F., (1984), *Physica Scripta*, **T7**, 157
75. Edge A.C., Stewart G.C., (1991), *Mont. No. R. Astr. Soc.*, **252**, 414